

Characterization and Dielectric Study of Mihaliccik Tremolite

Ertugrul Izci

Physics Department, Science Faculty, Eskisehir Technical University, Eskisehir, Turkey

ABSTRACT

The natural tremolite $\text{Ca}_2\text{Mg}_5\text{Si}_8\text{O}_{22}(\text{OH})_2$ was obtained from Mihaliccik district of Eskisehir, Turkey (39.8787N; 31.3806E). It is a part of the amphibole family of silicate minerals. All the phases were described by X-ray diffraction (XRD), energy dispersive spectroscopy (EDXRF), Raman, and Fourier transform infrared spectroscopy (FTIR). The natural tremolite specimen used in this study includes mostly 54.4% SiO_2 , 22.82% MgO , 15.04% CaO , and 1.45% Al_2O_3 . The natural tremolite sample used for the present investigation was not pure. The impurity was calcite. The FTIR spectrum and the Raman spectrum were recorded for natural tremolite sample in the range of 4000 and 350 cm^{-1} and 4000 and 70 cm^{-1} at room temperature, respectively. The natural tremolite and fired tremolite samples were prepared for this investigation. Dielectric measurements were realized in the 3 kHz – 1 MHz frequency region and at the room temperature by using HP4192A LF Impedance Analyzer. The dielectric parameters of the samples were obtained; the conclusions of the study were explained and given to be used for further investigations in some industrial productions.

KEYWORDS: Tremolite; XRD, spectroscopy, dielectric properties

INTRODUCTION

Tremolite $\text{Ca}_2\text{Mg}_5\text{Si}_8\text{O}_{22}(\text{OH})_2$ is an end-member of the calcic amphibole family of silicate minerals [1-6]. Calcic amphiboles crystallize in the monoclinic crystal system, space group C2/m [7-10]. They have tetrahedral, octahedral, and eight coordinated cation sites. These cation sites (M1, M2, and M3) are octahedrally coordinated whereas M4 sites are surrounded by eight anions [7,10,11]. The crystal structures of them are characterized by double silicate chains linked together by strips of M^{2+} cations. The M1 and M2 sites of tremolite are fully occupied by Mg^{2+} , the M3 site by Mg^{2+} or/and Fe^{2+} and the M4 site by Ca^{2+} [8,10-14]. All of the amphiboles, and specifically tremolite, are very durable to chemical assault by powerful acids and bases [1,3,10]. But they have many disadvantages such as large production of hazardous waste and risk of environmental contamination during and after the process [15]. When they are fired at temperatures higher than 1100°C , they show the changes in the microstructure and technological features and transform into Mg- or Fe- silicates and new products can be obtained. At elevated temperatures, 1250°C , the structures of them change and enstatite (MgSiO_3), diopside ($\text{CaMgSi}_2\text{O}_6$), quartz (SiO_2), and water result from them breakdown [12]. The final products do not have risk of environmental pollution and decreased of possibilities of exposure for employees concerned with the disposal processes [15].

Dielectric properties of materials have attracted both theoreticians and experimentalists for more than a century [16]. High dielectric constant materials have technologically substantial because of their promising effects on microelectronic apparatus applications [17]. The complex permittivity defines the whole interplay of the dielectric

How to cite this paper: Ertugrul Izci "Characterization and Dielectric Study of Mihaliccik Tremolite" Published in International Journal of Trend in Scientific Research and Development (ijtsrd), ISSN: 2456-6470, Volume-4 | Issue-1, December 2019, pp.749-756, URL: www.ijtsrd.com/papers/ijtsrd29671.pdf



IJTSRD29671

Copyright © 2019 by author(s) and International Journal of Trend in Scientific Research and Development Journal. This is an Open Access article distributed under the terms of the Creative Commons Attribution License (CC BY 4.0) (<http://creativecommons.org/licenses/by/4.0>)



materials with the changeable electrical field. In this instance, the following equation is used:

$$Y = j(\epsilon_r' - j\epsilon_r'')\omega C_0 = G_p + jB_p$$

Equating imaginary part of admittance gives conductance

$$G_p = \epsilon_r''\omega C_0$$

and real part of it gives susceptance [17,18].

$$B_p = \epsilon_r'\omega C_0$$

where ω is the angular frequency, $2\pi f$, and f is called frequency. The tangent of the loss angle, δ , mostly called the loss tangent [18] and it is described as

$$\tan\delta = \frac{\epsilon_r''}{\epsilon_r'}$$

In spite of the fact that there have been some investigations on the dielectric properties of the fired or not fired materials especially ceramics [19-22], a comprehensive investigation of the effects of firing temperatures on the permittivity and loss tangent of tremolite sample has not been realized.

In the literature, there are many investigations on the structural analysis of tremolite sample collected from different regions of the world using XRD, EDXRF, FTIR and Raman spectroscopy. The purpose of this investigation is to recognize the major and minor phases, to define structurally tremolite sample using these techniques and to investigate the permittivity and loss tangent of tremolite samples that were fired at different temperatures.

EXPERIMENTAL

The natural tremolite sample was collected from Mihalıcık region in Turkey (39.8788N; 31.3806E).

Powder XRD pattern of the natural tremolite sample was obtained on a Rigaku DMAX diffractometer equipped with $\text{CuK}\alpha$ radiation of the XRD Laboratory, Material Science and Engineering Department, Eskisehir Technical University. Operating conditions for this sample was 40 kV and 30 mA. The 2θ (2 θ) scanning range was between 10° and 70° and the scanning speed was $4^\circ/\text{min}$.

Powdered natural tremolite sample was prepared by grinding about 10 mg of sample in an agate mortar. 2.5 mg of the natural tremolite sample was homogenized with 250 mg of KBr by grinding in an agate mortar. The mixture was pressed at 5 ton for 3 min using a hydraulic hand press in an evacuated die into a 13 mm pellet. The discs were dried at 120°C for 3 h. The FTIR spectra using the KBr pellet method were recorded with the Bruker IFS 66 v/S FTIR system in the spectral range $350\text{--}4000\text{ cm}^{-1}$. The Raman spectra of the natural tremolite sample were acquired with a Bruker Senterra Dispersive Raman microscope spectrometer using 532 nm excitation in the spectral range $70\text{--}3700\text{ cm}^{-1}$. The Raman and FTIR spectra were recorded at the Raman and Infrared Spectroscopies Laboratory, Physics Department, Eskisehir Technical University.

The tremolite discs used for dielectric measurements were prepared as follows: Firstly, the natural tremolite sample was ground using a mortar. Then, the powder natural tremolite sample pressed into discs with a thickness of 0.693 ± 0.082 mm and diameter of 12 mm. Finally, the discs were fired at various temperatures for 1 h by furnace cooling down to room temperature [20,22]. Electrodes were made by sputtering a platinum film on both sides of the discs. Dielectric properties, including conductance (G) and susceptance (B), were obtained using an HP 4194A LF Impedance Analyzer at room temperature. Measuring frequencies were varied from 1.10^3 to 1.10^6 Hz. The dielectric permittivity (ϵ') and loss tangent ($\tan\delta$) values were determined at these measuring results.

RESULTS AND DISCUSSION

A. Chemical Analysis and X-ray Powder Diffraction

The natural tremolite sample used in this investigation includes principally 54.41% SiO_2 , 22.81% MgO , 15.04% CaO , and 1.45% Al_2O_3 , 1.42% Na_2O , 0.18% FeO , and 4.69% others & H_2O .

As shown in Fig. 1, the natural tremolite sample occurs of tremolite with minor amount of calcite. The characteristic XRD peaks are appeared at $2\theta = 28.60$, 10.540 , and 27.240 for tremolite, at 29.380 , 22.980 , and 48.720 for calcite in the present investigation.

B. FTIR Spectroscopy

The mineralogical investigation of natural tremolite sample was determined with the help of FTIR spectroscopy. The FTIR spectrum over the $350\text{--}1200\text{ cm}^{-1}$ spectral range is reported in Fig. 2. As is illustrated in Fig. 2, a series of overlapping FTIR peaks are identified at 1063, 1020, 997, 952, and 919 cm^{-1} . The first four peaks are ascribed to antisymmetric stretching vibrations of the Si-O-Si [3] and the peak at 919 cm^{-1} is attributed to the symmetric stretching

vibration of Si-O-Si bond [24]. The infrared peaks at 1105, 875, 713, and 445 cm^{-1} is assigned to the CO_3^{2-} vibrations of calcite [3, 25, 26].

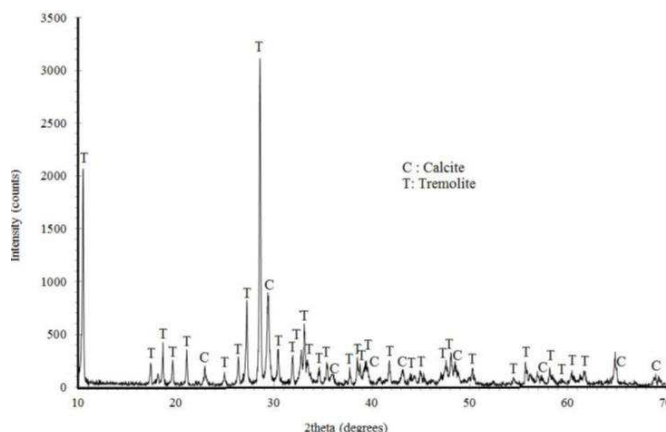


Figure1. XRD peaks of the Mihalıcık tremolite sample.

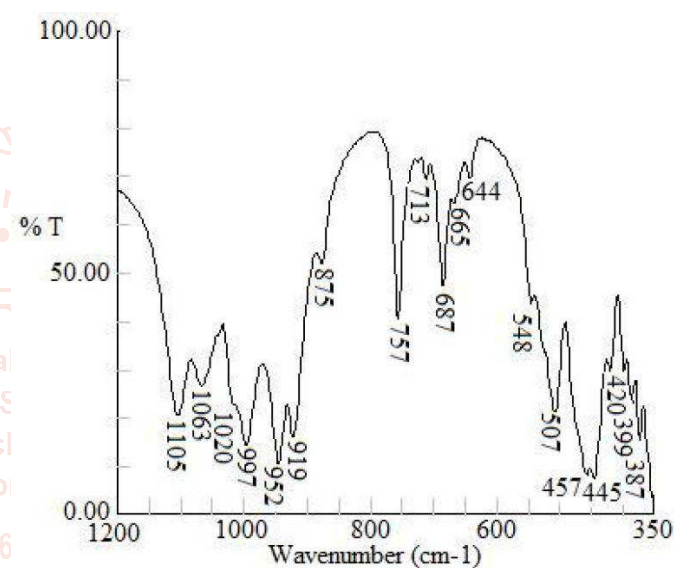


Figure2. FTIR spectrum of the natural tremolite sample (in the $350\text{--}1200\text{ cm}^{-1}$ range)

The infrared peaks shown at 687 and 757 cm^{-1} are attributed to the symmetrical stretching of Si-O-Si bending [3, 24]. The peaks at 457, 507, and 548 cm^{-1} are ascribed to the bending vibrations of the Si-O-Si. Also, the infrared peaks at 387, 399, and 420 cm^{-1} are attributed to the M-O (metal-oxygen) stretching vibrations [3,25]. These peaks provide the first positive evidence of the presence of calcite in the sample [3,26].

As can be seen from Fig. 3, the FTIR spectrum of the natural tremolite sample around 3669 cm^{-1} includes a complex property consisted of several peaks, all of which are assignable to OH stretching vibrations [11,14,25,27]. In this spectrum, the peaks at 2881, 2644, 2497, 1794, and 1417 cm^{-1} show the presence of calcite in the natural tremolite sample. The peak at 1417 cm^{-1} is ascribed to Ca-O asymmetric stretching vibration. Also, the other peaks are ascribed to C-O symmetric stretching vibrations [26]. The data are summarized in Table 1.

As can be seen from Fig. 3, the FTIR spectrum of the natural tremolite sample around 3669 cm^{-1} includes a complex property consisted of several peaks, all of which are assignable to OH stretching vibrations [11,14,25,27]. In this spectrum, the peaks at 2881, 2644, 2497, 1794, and 1417 cm^{-1}

cm⁻¹ show the presence of calcite in the natural tremolite sample. The peak at 1417 cm⁻¹ is ascribed to Ca- O asymmetric stretching vibration. Also, the other peaks are

ascribed to C-O symmetric stretching vibrations [26]. The data are summarized in Table 1.

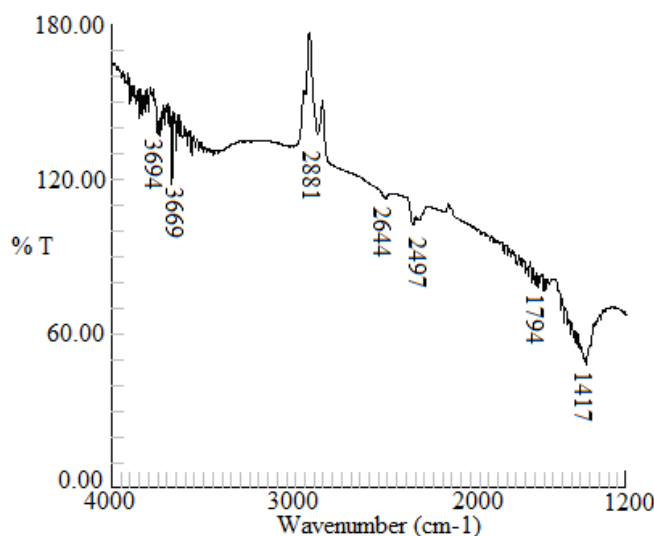


Figure3. FTIR spectrum of the natural tremolite sample (in the 1200 - 4000 cm⁻¹ range)

TABLE1. Band assignments for the peaks obtained for Mihaliccik tremolite

Tentative Assign.	This work cm ⁻¹	Makreski et al. cm ⁻¹	Shurvell et al. cm ⁻¹	Taylor et al. ^{a,b} cm ⁻¹
νs(OH)	3694	3690	-	-
νs(OH)	3669	3673	-	-
νs(OH)	-	3659	-	-
Calcite	2881	-	-	-
Calcite	2644	-	-	-
Calcite	2497	-	-	-
Calcite	1797	-	-	-
Calcite	1417	-	-	-
Calcite	1105	1100	1106	1100
νas(Si-O-Si)	1063	-	1057	1050
νas(Si-O-Si)	1020	1017	1017	1016
νas(O-Si-O)	997	995	998	992
νas(Si-O-Si)	952	953	953	955
νs(Si-O-Si)	919	920	922	918
Calcite	875	-	-	-
νs(Si-O-Si)	757	757	758	753
Calcite	713	-	-	-
νs(Si-O-Si)	687	684	686	682
νs(Si-O-Si)	665	669	664	-
νs(Si-O-Si)	644	643	643	-
δ(Si-O-Si)	-	603	-	593
δ(Si-O-Si)	-	583	-	-
δ(Si-O-Si)	548	542	546	-
δ(Si-O-Si)	507	507	509	508
δ(Si-O-Si)	-	465	468	465
δ(Si-O-Si)	457	454	-	450
Calcite	445	443	448	-
T(M-OH)	420	420	420	420
T(M-OH)	399	401	-	400
T(M-OH)	387	387	-	388

M: Mg²⁺, Fe²⁺, Ca²⁺

^a: Intensities are not given

^b: Stretching OH vibrations are not studied [24].

C. Raman Spectroscopy

Fig. 4 shows the Raman spectrum of the natural tremolite in the range of 70 and 500 cm⁻¹. Six peaks which are ascribed to lattice vibrations appear at 79.5, 118, 149.5, 159, 177.5, and 248 cm⁻¹ [9,28]. O-H-O vibrations produce one other strong peak at about

222.5 cm^{-1} . The 286 cm^{-1} peak is ascribed to the vibration between cation and oxygen (M-O) of the CO_3 group and this peak is characteristic peak of calcite [29,30]. Similarly, the peak at 368.5 cm^{-1} is due to the Fe-OH vibration and the peak at 411 cm^{-1} can be assigned to Mg-OH [9]. In the 300- 450 cm^{-1} , these vibrations are produced by Ca^{2+} , Mg^{2+} , and/ or Fe^{2+} cations. The octahedral positions on tremolite are normally occupied by Ca^{2+} , Mg^{2+} and Fe^{2+} cations linked to OH- groups but at this region, the assignments of the M- O vibrations are suspect [9,31,32].

Fig. 5 shows Raman spectrum in the 500- 1150 cm^{-1} range. In the spectral region 1150-500 cm^{-1} , four significantly intense bands at 1058, 1028, 925 and 674 cm^{-1} , and three weak peaks at 740, 602, 532 cm^{-1} are observed. The most intense Raman peak is found at 674 cm^{-1} and it is assigned to the symmetric stretching (vs) of the Si-O-Si bridges. The peaks at 740 and 925 cm^{-1} are produced by the symmetric stretching vibrations of the Si- O- Si groups. the peaks observed at 1028 and 1058 cm^{-1} in this spectrum are assigned to antisymmetric stretching mode of Si- O- Si [28,31,32]. Two peaks at 1085 and 703 cm^{-1} in the spectrum are related to the calcite. The first peak at 1085 cm^{-1} is assigned to symmetric stretching of the CO_3 group. Also, the second peak is assigned to the bending mode of the CO_3 group [9,28,32].

The Raman spectrum over the 3500- 3700 cm^{-1} spectral range is reported in Fig. 6. The spectrum exhibits a very strong band centered at 3673 cm^{-1} and a weak band at 3615 cm^{-1} as due to O-H stretching vibrations. The number and relative intensity of these peaks depend on the Fe^{2+} or Mg^{2+} . When only Mg is present (as in pure tremolite), only one peak (at 3673 cm^{-1}) is observed [25,33]. The Raman peaks are listed in Table 2 with possible assignments in order to define the spectral features.

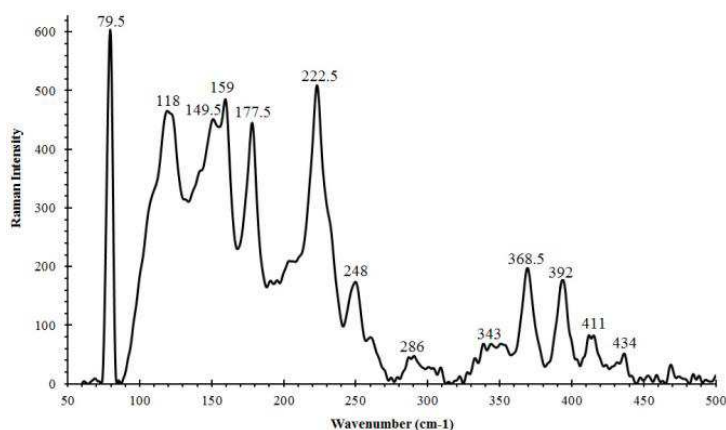


Figure4. A Raman spectrum of the natural tremolite sample (in the 50- 500 cm^{-1} spectrum range)

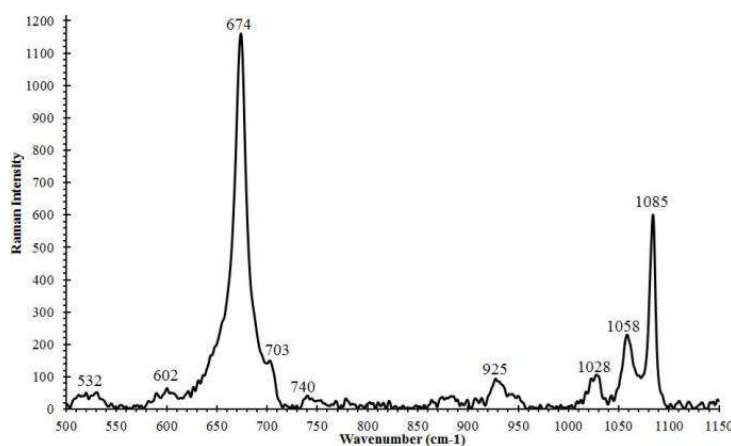


Figure5. A Raman spectrum of the natural tremolite (in the region 500- 1150 cm^{-1})

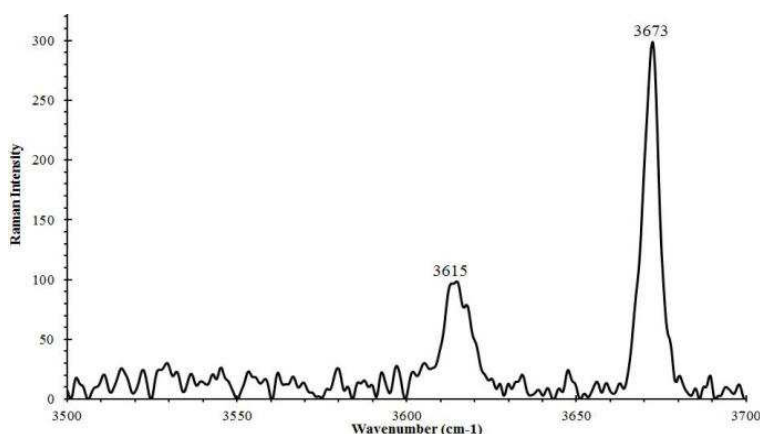


Figure6. A Raman spectrum (between 3500- 3700 cm^{-1}) of the Mihaliccik tremolite

TABLE2. Wave numbers and assignments for the Raman spectrum of Mihaliccik tremolite in the 70- 3700 cm⁻¹ spectral region

Tentative Assignment	This study cm ⁻¹	Apopei et al. [9] cm ⁻¹	Bard et al. [18] cm ⁻¹
vs(OH)	3673	-	3677
vs(OH)	3615	-	-
vs of CO ₃ (calcite inclusions)	1085	1083	-
vas(Si- O- Si)	1058	1059	1061
vas(Si- O- Si)	1028	1027	1028
vs(Si- O- Si)	925	928	928
vs(Si- O- Si)	740	747	-
vbending of CO ₃ (calcite inclusions)	703	-	711
vs(Si- O- Si)	674	674	672
Deformation mode of Si ₄ O ₁₁	532	525	-
M-O (M= Mg ²⁺ and Fe ²⁺)	434	438	-
M-O (M= Mg ²⁺ and Fe ²⁺)	411	415	414
M-O (M= Mg ²⁺ and Fe ²⁺)	392	394	393
M-O (M= Mg ²⁺ and Fe ²⁺)	368.5	369	369
M-O (M= Mg ²⁺ and Fe ²⁺)	343	349	349
M-O (M= Ca ²⁺) (calcite inclusions)	286	285	-
Lattice mode	248	250	251
O- H- O vibration	222.5	226	222
Lattice mode	177.5	-	-
Lattice mode	159	-	-
Lattice mode	149.5	-	-
Lattice mode	118	-	-
Lattice mode	79.5	-	-

D. Dielectric Properties

The variation of the permittivity, ϵ' , with log frequency at different firing temperatures between 200 and 1200 °C is shown in Fig. 7. As can be seen from Fig. 7, at frequencies between 3 kHz and 1 MHz, the permittivity (ϵ') is in the range of 3.48– 6.18 at different firing temperatures between 400 and 1200 °C. The permittivity of natural tremolite at 20 °C is 7.03 [38]. It is known to be a member of low permittivity dielectrics because its permittivity values are lower than 15 and because of these properties; it is widely used for straightforward insulation due to these properties [39]. The permittivity decreases gradually with an increase in firing temperatures up to 400 °C. It is seen that the permittivity (ϵ') decreases with an increase in log frequency at all the firing temperatures. This is a normal behavior of dielectric materials. Displacement of charge carriers occurs in tremolite, which is a dielectric material, under the influence of an applied electric field. The process of dipole alignment is known as polarization. The total polarization of the dielectric material can be represented as the sum of four polarizations which are called the electronic, ionic, dipolar, and space charge polarizations. Dielectric material exhibits at least one of these polarization types. This depends on the bonding and structure of the material, and the frequency [4,40,41].

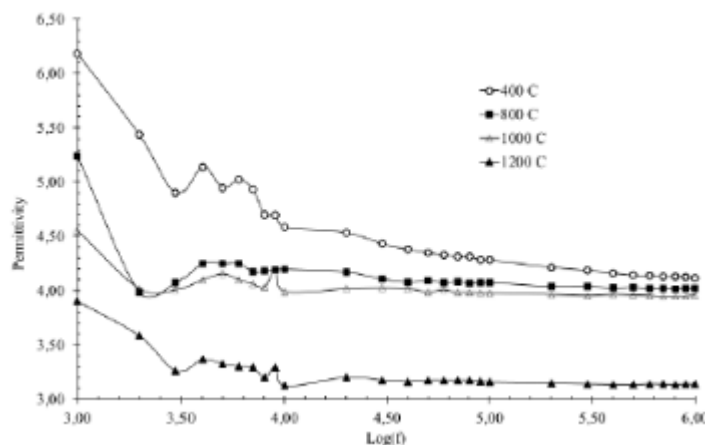


Figure7. Frequency dependence of the permittivity at different firing temperatures of tremolite

Fig. 8 shows the variation of the loss tangent, $\tan\delta$, with log frequency at different firing temperatures between 400 and 1200 °C for tremolite at room temperature. This variation is like the variation of permittivity with log frequency. It is

observed that both permittivity and loss tangent decreased with frequency which is one of the features of polar dielectrics [42]. The loss tangent, $\tan\delta$, decreases from 0.046 to 0.014 when log frequency is increased from 5.00 to 6.00, at

different firing temperatures. At 6.6 MHz frequency, loss tangent of firing tremolite at 1200 °C sharply increases due to the tremolite property. The dielectric losses are due to ionic conduction, particularly at low frequencies, and rotation of permanent dipoles at higher frequencies [43].

Fig. 9 shows the variation of the permittivity, ϵ' , with firing temperatures between 200 and 1200 °C at 0.1 MHz, 1 MHz and 10 MHz frequencies. From the graph, the permittivity increases gradually in firing temperatures below 400 °C. The value of permittivity is constant during firing from 400 to 1000 °C and it decreases at firing temperatures from 1000 to 1200 °C. When tremolite is fired at temperatures over 1000 °C, it transforms into Mg – silicate. As a result, the permittivity value decreases sharply at 1200 °C, its value is minimum for 1, 5 and 10 MHz frequencies. The loss tangent of each sample fired at temperatures from 200 up to 1200 °C is graphically plotted as a function of firing temperature in Fig. 10. The loss tangent values for these samples increase with firing temperatures between 200 and 400 °C and at 0.1 MHz frequency; the loss tangent of tremolite sample has maximum value at firing temperature of 400 °C at room temperature. The loss tangent values of samples decrease as the firing temperature increases from 400 to 1000 °C at room temperature. Then, stable loss tangent values were observed with increasing temperature at room temperature. The decomposition temperature of tremolite was between 950 and 1040 °C and its fusion temperature of it was 1224 °C [43-46]. The obtained results in Fig. 9 and 10 are consistent with the results of research conducted by Vijayasree et al. [46].

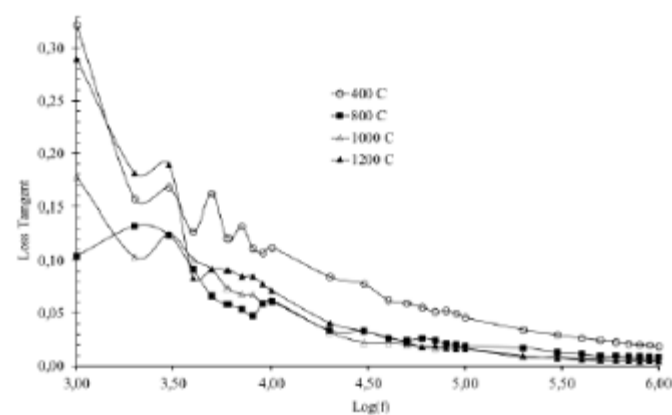


Figure8. Frequency dependence of the loss tangent at different firing temperatures of tremolite

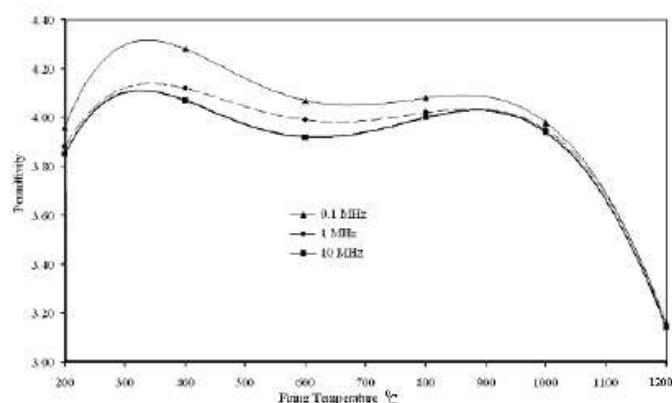


Figure9. Dependence of permittivity on firing temperature of tremolite at room temperature for constant frequencies (0.1 MHz, 1 MHz and 10 MHz)

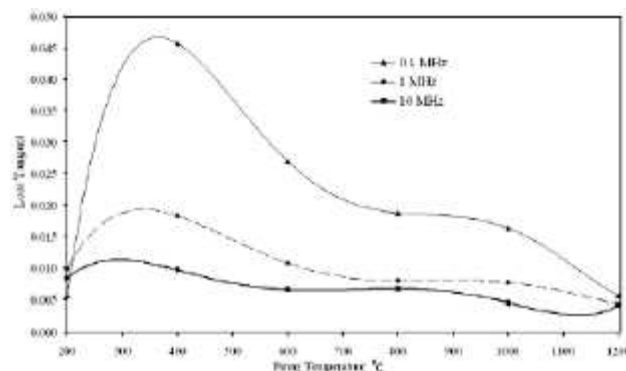


Figure10. Dependence of loss tangent on firing temperature of tremolite at room temperature for constant frequencies (0.1 MHz, 1 MHz and 10 MHz)

CONCLUSION

In this paper, XRD pattern shows that natural tremolite sample has very strong peaks of tremolite (T), and a low intensity of the peaks of calcite (C) and contains tremolite as a major mineral and calcite as impurity. To understand in chemical composition and structure of the natural tremolite sample were used by Raman and FTIR spectroscopies and EDXRF analyses. Raman and FTIR spectra contain the characteristic bands of tremolite and calcite, in accordance with XRD result.

The applied frequency and firing temperature affect the dielectric properties. The permittivity values of tremolite range from 3.90 to 6.18 depending on the firing temperatures at 1 kHz frequency. Tremolite is a dielectric material and it is a member of low permittivity dielectrics ($\epsilon' < 15$). It can widely use for straightforward insulation and it can find some applications as capacitor dielectrics where very small capacitances are required for use at higher frequencies.

Acknowledgment

I thank to Res.Asst. Dr. O. Baglayan for recording Raman and FTIR spectra and Havva D. Unluce for recording the XRD pattern.

References:

- [1] J. Addison and E.E. McConel, "A review of carcinogeny studies of asbestos and non-asbestos tremolite and other amphiboles," Regul. Toxicol. Pharmacol, vol. 52(Suppl 1), pp. 87-199, 2008.
- [2] K. Ishida, D. M. Jenkins, and F. C. Hawthorne, "Mid-IR bands of synthetic calcic amphiboles of tremolite-pargasite series and of natural calcic amphiboles," Am. Mineral, vol 93(7), pp. 1112-1118, 2008.
- [3] K. W. Ryu, M. G. Lee, and Y.G. Jang, "Mechanism of tremolite carbonation," Appl. Geochem, vol. 26(7), pp. 1215-1221, 2011.
- [4] N. M. Johnson and J. B. Fegley, "Water on Venus: new insights from tremolite decomposition," Icarus, vol. 146(1), pp. 301-306, 2000.
- [5] F. C. Hawthorne and G. D. Ventura, "Short-range order in amphiboles," Rev. Mineral. Geochem. vol. 67(1) pp. 173- 222, 2007.
- [6] M. Ristic, I. Czako – Nagy, S. Music, and A. Vertes, "Spectroscopic characterization of chrysotile asbestos from different regions," J. Mol. Struct, vol. 993(1-3), pp. 120-126, 2011.

- [7] E. T. Schmidbauer, T. Kunzmann, T. Fehr, and R. "Hochleitner, Electrical resistivity and ^{57}Fe Moessbauer spectra of Fe-bearing calcic amphiboles," *Phys. Chem. Miner.*, vol. 27, pp. 347–356, 2000.
- [8] A. I. Apopei, N. Buzgar, and A. Buzatu, "Raman and infrared spectroscopy of kaersutite and certain common amphiboles," *A.U.I. Geologie*, vol.57, vol. 35 – 58, 2011.
- [9] A.I. Apopei, and N. Buzgar, "The Raman study of amphiboles," *A. I. I. Cuza Geologie*, vol. 1, pp. 57–83, 2011.
- [10] M. Ross, A. M. Langer, G.L. Nord, R. P. Nolan, R. J. Lee, D. V. Orden, and J. Addison, "The Mineral nature of asbestos," *Regul. Toxicol. Pharm.*, vol. 52, pp. 26–30, 2008.
- [11] M. Gottschalk, M. Andrut, and S. Melzer, "The Determination of the cummingtonite content of synthetic tremolite," *Eur. J. Mineral*, vol. 11, pp. 967–982, 1999.
- [12] N. M. Johnson and J. B. Fegley, "Tremolite decomposition Venus II products, kinetics, and mechanism," *Icarus*, vol. 164, pp. 317–333, 2003.
- [13] M. Andrut, M. Gottschalk, S. Melzer, and J. Najorka, "Lattice vibrational modes in synthetic tremolite-Sr-tremolite and tremolite- richterite solid solutions," *Phys. Chem. Miner.*, vol. 27, pp. 301–309, 2000.
- [14] J. Najorka J and M. Gottschalk, "Crystal chemistry of tremolite – tschermakite solid solution," *Phys. Chem. Miner.* Vol. 30, pp. 108–124, 2003.
- [15] A. F. Gualtieri and A. Tartaglia, "Thermal decomposition of asbestos and recycling in traditional ceramics," *J. Eur. Ceram. Soc.*, vol. 20, pp. 1409–1418, 2000.
- [16] E. Tuncer, N. Bowler, I.J. Youngs, and K. P. Lymer, "Investigating low frequency dielectric properties of a composite using the distributing of relaxation times technique," *Philos. Mag.*, vol. 86(16), pp. 2359–2369, 2006.
- [17] J. Li, K. Cho, N. Wu, and A. Ignatiev, "Correlation between dielectric properties and sintering temperatures of polycrystalline $\text{CaCu}_3\text{Ti}_4\text{O}_{12}$," *IEEE. Trans. Dielectr. Electr. Insul.*, vol.11 (3), pp. 534–541, 2004.
- [18] E. Barsoukov and J. R. Macdonald, *Impedance Spectroscopy Theory, Experiment, and Applications*. 2nd ed. Hoboken, NJ, USA, John Wiley & Sons, 2005.
- [19] C. T. Dervos, J. A. Mergos, and A. A. Iosifides, "Characterization of insulating particles by dielectric spectroscopy: case study for CaCO_3 powders," *Mater. Lett.*, vol. 59, pp. 2842–2849, 2005.
- [20] H. Zıpkın, L. Israel, S. Güler, and C. Güler, "Dielectric properties of sodium fluoride added kaolinite at different firing temperatures," *Ceram. Int.*, vol. 33, pp. 663–667, 2007.
- [21] G. H. Chen and X. Y. Liu, "Sintering, crystallization and properties of $\text{MgO-Al}_2\text{O}_3\text{-SiO}_2$ system glass - ceramics containing ZnO ," *J. Alloys. Compd.*, vol.431, pp. 282–286, 2007.
- [22] A. Kirak, H. Yılmaz, S. Güler, and C. Güler, "Dielectric properties and electric conductivity of talc and doped talc," *J. Phys. D. Appl. Phys.*, vol. 32, pp. 1919–1927, 1999.
- [23] D. M. Jenkins, T. J. B. Holland, and A. K. Clare, "Experimental determination of the pressure-temperature stability field and thermo chemical properties of synthetic tremolite," *Am. Mineral*, vol. 76, pp. 458–469, 1991.
- [24] N. O. Gopal, K.V. Narasimhulu, and J. L. Rao, "EPR, optical, infrared and Raman spectral studies of actinolite mineral," *Spectrochim. Acta. A*, vol. 60, pp. 2441–2448, 2004.
- [25] D. Bard, J. Yarwood, and B. Tylee, "Asbestos fibre identification by Raman micro spectroscopy," *J. Raman Spectrosc.*, vol. 28, pp. 803–809, 1997.
- [26] S. Gunasekaran and G. Anbalagan, "Spectroscopic study of phase transitions in natural calcite mineral," *Spectrochim. Acta. A*, vol. 69, pp. 1246–1251, 2008.
- [27] A. Pacella, G. B. Andreozzi, and J. Fournier, "Detailed crystal chemistry and iron topochemistry of asbestos occurring in its natural setting: A first step to understanding its chemical reactivity," *Chem. Geol.*, vol. 277, pp. 197–206, 2010.
- [28] P. Makreski, G. Jovanovski, and A. Gajovis, "The minerals from Macedonia: XVII. vibrational spectra of common appearing amphibole minerals," *Vib. Spectrosc.*, vol. 40, pp. 98–109, 2006.
- [29] I. Ozkaya, "Origin of asbestos occurrences in Mihalıcık (Eskisehir) region," *Bull. Geol. Soc. Turkey*, vol. 19, pp. 53– 58, 1975.
- [30] M. Akbulut, O. Piskin, and A. I. Karayigit, "The genesis of the carbonized and silicified ultramafic known as listvenites: a case study from the Mihalıcık Region (Eskisehir), NW Turkey," *Geol. J.*, vol.41, pp. 557–580, 2006.
- [31] C. Rinaudo, E. Belluso, and D. Gastaldi, "Assessment of the use of Raman spectroscopy for the determination of amphibole asbestos," *Mineral Mag* 2004; 68: 455–465.
- [32] J. Jehlicka, P. Vitek, H. G. M Edwards, M. Heagraves, and T. Capoun, "Application of portable Raman instruments for fast and non-destructive detection of minerals on outcrops," *Spectrochim Acta A* 2009; 73: 410–419.
- [33] R. Petry, R. Mastalerz, S. Zahn, T.G. Mayerhofer, G. Volksch, L. Viereck – Gotte, B. Kreher- Hartmann, L. Holz, M. Lankers, and J. Popp, "Asbestos mineral analysis by UV Raman and energy-dispersive x-ray spectroscopy," *Chemphyschem* 2006; 7: 414–420.
- [34] A. F. Gualtieri, N. B. Gandolfia, S. Pollastria, R. Rinaldia, O. Salaa, G. Martinellib, T. Baccib, F. Paolib, A. Vianic, and R. Vigliaturod, "Assessment of the potential hazard represented by natural raw materials containing mineral fibres - the case of the feldspar from Orani, Sardinia (Italy)," *J Hazard Mater* 2018; 350: 76–87.
- [35] I. K. Sadło, G. Gil, P. Gunia, M. Horszowski, and M. Sitarz, "Raman and FTIR spectra of nephrites from the Żłoty Stok and Jordanów Śląski (the Sudetes and Fore-Sudetic Block, SW Poland)," *J Mol Struct* 2018; 1166:

- 40-47.
- [36] M. C. Dichicco, A. De Bonis, G. Mongelli, G. Rizzo, and R. Sinisi, "μ-Raman spectroscopy and x-ray diffraction of asbestos' minerals for geo-environmental monitoring: The case of the southern Apennines natural sources," *Appl Clay Sci* 2017; 141: 292–299.
- [37] M. Hoehse, D. Mory, S. Florek, F. Weritz, I. Gornushkin, and U. Panne, "A combined laser-induced breakdown and Raman spectroscopy Echelle system for elemental and molecular microanalysis," *Spectrochim. Acta. Part. B*, vol. 64, pp. 1219–1227, 2009.
- [38] I. J. Rosenholtz and D.T. Smith, "The dielectric constant of mineral powders," *Am. Mineral*, vol. 21, pp. 115-120, 1936.
- [39] A. J. Moulson and J. M. Herbert, *Electro ceramics Materials, Properties, Applications*, 2nd ed., London, UK: Chapman & Hall, 1990.
- [40] R. N. P. Choudhary, D. K. Pradhan, G. E. Bonilla, R. S. Katiyar, "Effect of La-substitution on structural and dielectric properties of Bi(Sc_{1/2}Fe_{1/2})O₃ ceramics," *J. Alloys. Compd*, vol. 437(1–2), pp. 220–224, 2007.
- [41] A. A. Hodgson, "Nature and paragenesis of asbestos minerals," *Phil. Trans. R. Soc. Lond. A*, vol. 286, pp. 611– 624, 1977.
- [42] P. S. Das, P. K. Chakraborty, B. Behera, and R. N. P. Choudhary, "Electrical properties of Li₂BiV₅O₁₅ ceramics," *Physica. B. Condensed. Matter*, vol. 395, pp. 98–103, 2007.
- [43] C. Leonelli, P. Veronesi, D. N. Boccaccini, M. R. Rivasi, L. Barbieri, F. Andreola, I. Lancellotti, D. Rabitti, and G. C. Pellacani, "Microwave Thermal Inertisation of Asbestos Containing Waste and its Recycling in Traditional Ceramics," *J. Hazard. Mater*, vol. B135, pp. 9 – 155, 2006.
- [44] T. Diedrich, J. Achott, and H. Oelkers, "An experimental study of tremolite dissolution rates as a function of pH and temperature: Implications for tremolite toxicity and its use in carbon storage," *Mineral. Mag*, vol. 78(6), pp. 1449–1464, 2014.
- [45] A. Bloise, R. Kusiorowski, and A.F. Gualtieri, "The Effect of Grinding on Tremolite Asbestos and Anthophyllite Asbestos," *Mineral*, vol. 8 (274), pp. 1- 13, 2018.
- [46] G. Vijayasree, P. S. Mukherjee, and R. Bhattacharjee, "Dielectric properties of fibrous amphibole," *Indian. J. Phys*, vol. 50, pp. 1052-1056, 1970.

